Available online at www.sciencedirect.com
SCIENCE DIRECT
Journal of Catalysis 237 (2006) 416–425
JOURNAL OF CATALYSIS
www.elsevier.com/locate/jcat

Catalytic and multinuclear MAS NMR studies of a thermally treated zeolite ZSM-5

J. Kanellopoulos [a], A. Unger [b], W. Schwieger [b,*], D. Freude [a,*]

[a] *Fakultät für Physik und Geowissenschaften, Universität Leipzig, 04103 Leipzig, Germany*
[b] *Institute of Chemical Reaction Engineering, University of Erlangen-Nuremberg, 91058 Erlangen, Germany*

Received 9 March 2005; revised 7 October 2005; accepted 23 November 2005

Abstract

Catalysts of ZSM-5 type were obtained by synthesis with tetrapropyl-ammonium-bromide (TPABr) as a template and subsequent hydrothermal treatment up to 1173 K. ^{1}H-, ^{27}Al-, and ^{29}Si-NMR spectroscopy and the direct oxidation of benzene with N_2O as a catalytic test were applied to characterize the products. ^{27}Al MAS NMR and ^{27}Al 3QMAS NMR studies of the samples give evidence that fivefold-coordinated extra-framework aluminum species exist if the product is treated at 1173 K and then rehydrated. The values of all characteristic catalytic key data are highest when the catalysts are precalcined at 1173 K. This is a clue that species giving rise to fivefold-coordinated aluminum species in the hydrated products are responsible for the high catalytic key data. The nature of these species is not yet clear. Two models for the species are in agreement with our experimental findings.

Keywords: ZSM-5; Hydrothermal treatment; Catalytic test; ^{1}H MAS NMR; ^{27}Al MAS NMR; 3QMAS NMR; Exchange spectroscopy

1. Introduction

Dealumination of zeolites enhances the acid strength of catalytic Brønsted sites, reducing the concentration of Brønsted sites and thus the rate of the coking process. In addition, it creates extra-framework aluminum species, which can act as Lewis acid sites in combination with the Brønsted sites [1]. The modification of ZSM-5 zeolite can alter the product distribution of the chemical reaction in, for example, the alkylation of benzene [2]. The chemical composition and structural aspects of solid acid catalysts can be characterized by inductively coupled plasma atomic emission spectroscopy (AES-ICP), X-ray diffraction (XRD), nitrogen adsorption, temperature-programmed desorption (TPD) of ammonia, and Fourier transformed infrared spectra (FTIR) of adsorbed pyridine.

Magic-angle spinning nuclear magnetic resonance (MAS NMR) has been largely applied for the investigation of catalytic sites and molecules adsorbed on catalysts [3,4]. ^{27}Al MAS NMR spectroscopy allows the determination of coordination and concentration of Al species. The triple-quantum (^{27}Al 3QMAS NMR) technique can be applied to improve the resolution of the signals [5]. ^{1}H MAS NMR spectroscopy of dehydrated zeolites in fused glass ampoules gives the concentrations of several OH species. Additional strong irradiation of the ^{27}Al resonance frequency [6] quenches the signal of OH species with dipolar coupling to ^{27}Al nuclei [7,8]. Dynamic properties of the Brønsted sites can be investigated by measuring the temperature-dependent rate of the hydrogen exchange (exchange spectroscopy [EXSY]) between the sites and adsorbed benzene molecules by means of a ^{1}H NOESY NMR pulse sequence [9]. All of these NMR techniques were also applied to physicochemical methods for characterizing modified zeolites; these modification steps are described in detail to present a complete characterization of catalyst preparation. The direct oxidation of benzene with N_2O in a lab-scale setup with a plug-flow reactor and an on-line chromatographic analysis for the reaction mixture [10] were applied to test the catalysts finally obtained.

* Corresponding author.
E-mail addresses: wilhelm.schwieger@tc.uni-erlangen.de (W. Schwieger), freude@uni-leipzig.de (D. Freude).

0021-9517/$ – see front matter
doi:10.1016/j.jcat.2005.11.030

2. Experimental

2.1. Zeolite synthesis

The synthesis of ZSM-5-type zeolites, which contain in their as-synthesized form TPA^+-cations and sodium cations, was carried out in a 2-L stirring autoclave through hydrothermal crystallization of a reaction mixture with Si/Al-ratios of 15 and 40 starting from sodium aluminate as the Al_2O_3 source, colloidal silicic acid as the SiO_2 source, and tetrapropylammonium-bromide (TPABr) as the template [11]. Two solutions were prepared, one by dissolving NaOH in distilled water and then adding sodium aluminate solution and the other by diluting silicic acid (Köstrosol 1030) with distilled water and then dissolving TPABr in it to give a clear solution. Both solutions were mixed and stirred at 550 rpm for 2 h, after which the resulting gel was transferred to the autoclave. Crystallization was carried out at a temperature of 448 K for 16 h. Then the zeolite was removed, was washed with distilled water, and dried in an oven at 383 K for 20 h.

2.2. Modification

Hydrogen forms of the zeolite were obtained by three treatments of the two synthesized Na forms, α and β. We denote the starting material Na–H-ZSM-5 with a framework Si/Al ratio of 16 by α and those with a Si/Al ratio of 24 by β. The procedures are denoted by I, II or III; the obtained products (for both starting materials α and β) are denoted by a (as-synthesized), b, c, d and e (see Table 1).

Procedure II, consisting of treatment steps 2, 3, and 4, corresponds to the well-established treatment procedure for an as-synthesized organic template-containing zeolite to prepare the acidic form of the zeolite [12–16]. It is well known [10,17,18] that catalysts for the hydroxylation of benzene to phenol should be pretreated at high temperatures; see step 4 in Table 1. Here we introduce procedures I and III. In procedure I we added an HCl acid treatment at room temperature before the start of the standard procedure. In procedure III we introduced the HCl treatment to reduce the alkalinity in the sample before NH_4 ion exchange, which was carried out without a calcination step in between. Finally, after the calcination at 823 K (treatment step 3), we applied calcination at 1173 K (treatment step 4) in all procedures. All samples were fully characterized after each treatment step; samples d and e were applied in the hydroxylation reaction of benzene to phenol with N_2O.

In what follows we let αIIe denote a H-ZSM-5 product obtained from the starting material α, which was treated by procedure II up to 1173 K, and let βa denote the as-synthesized form with a framework Si/Al ratio of 24.

2.3. Preparation of NMR samples

^{27}Al MAS NMR and ^{29}Si MAS NMR were generally carried out on rehydrated samples that had been kept in a desiccator for 48 h over aqueous NH_4Cl. For ^{1}H MAS NMR, samples were dehydrated by heating 6-mm-deep layers of zeolite in glass tubes (5 mm o.d.) at a rate of 10 K h^{-1} under vacuum. The samples were maintained at 673 K and $<10^{-2}$ Pa for 24 h, after which they were loaded under vacuum at room temperature and sealed off. The adsorption of O_2 at 13 kPa decreases the T_1 from the maximum value of 10–0.5 s, so that the MAS NMR spectra of the dehydrated samples could be acquired with only a 1-s recycle delay. Benzene-loaded samples contain about 1.3 benzene molecules per unit cell. (A unit cell consists of 96 T-atoms and 192 oxygen atoms.)

2.4. ICP, XRD, BET, TPD, and FTIR characterization

Chemical composition of the products was determined by inductively coupled plasma atomic emission spectroscopy (ICP-AES) using a Perkin–Elmer Plasma 400 emission spectrometer. XRD measurements were performed in an angle range of $2\theta = 5°$–$50°$ using a Phillips X'Pert diffractometer URD 63 with Cu-K_α radiation. The nitrogen adsorption isotherms were measured at 77 K using a Micromeritics ASAP 2000. BET surface areas and micropore product volumes were obtained from the adsorption isotherms at a thickness range of 5–7 Å. TPD of ammonia (NH_3-TPD) was investigated using an Altamira Instruments AMI-100. FTIR spectra of adsorbed pyridine species were obtained using a Perkin–Elmer VX 170 spectrometer.

2.5. Catalytic testing

The direct benzene oxidation with N_2O as catalytic screening was performed in a lab-scale setup with a plug-flow reactor and an on-line chromatography for the reaction mixture. Experiments were carried out at 723 K, a modified residence time of

Table 1
Modification procedures for the zeolites ZSM-5

	Procedure I	Procedure II	Procedure III
Product a	As-synthesized Na^+-TPA^+-ZSM-5 (α or β)		
Step 1	HCl acid treatment		HCl acid treatment
Product b	H–Na^+-TPA^+-ZSM-5		H-Na^+-TPA^+-ZSM-5
Step 2	3 h calcination at 823 K	3 h calcination at 823 K	
Product c	H–Na^+-ZSM-5	Na^+-ZSM-5	
Step 3	NH_4NO_3 ion exchange + 2 h calcination at 823 K	NH_4NO_3 ion exchange + 2 h calcination at 823 K	NH_4NO_3 ion exchange + 2 h calcination at 823 K
Product d	H-ZSM-5	H-ZSM-5	H-ZSM-5
Step 4	2 h calcination at 1173 K	2 h calcination at 1173 K	2 h calcination at 1173 K
Product e	H-ZSM-5	H-ZSM-5	H-ZSM-5

93 g min mol^{-1} ($m_{cat} = 2$ g), a N_2O/benzene ratio of 1 and a large helium excess. Then 1 g of 0.75- to 1-mm catalyst fraction was placed into the 17.4-mm-i.d. reactor. The experiments were performed for 3 h time on stream. The first chromatographic analysis was obtained 15 min after the reaction was started, and further measurements were done every 29 min thereafter. The detailed procedure for catalyst testing has been described previously [10].

2.6. NMR measurements

^{27}Al MAS measurements were performed on a Bruker MSL 500 spectrometer (external field, $B_0 = 11.74$ T; Larmor frequency, $\nu_L = 130$ MHz) and an Avance 750 ($B_0 = 17.25$ T; $\nu_L = 195$ MHz) with MAS frequencies of $\nu_{rot} = 10$ kHz for the MSL 500 and 30 kHz for the Avance 750. Nutation frequencies were about 100 kHz for the MSL 500 and 185 kHz for the Avance 750. 3QMAS spectra were obtained using Avance 400 and Avance 750 spectrometers with an MAS frequency of 30 kHz. As a reference for the ^{27}Al intensity measurements, a well-characterized sample of H-ZSM-5 with a framework Si/Al ratio of 17 was used. ^{27}Al MAS NMR spectra were fitted using the dmfit program [19]. ^{29}Si MAS NMR investigations of the starting materials α and β gave Si/Al ratios in accordance with the values determined by ^{27}Al MAS NMR.

^{1}H MAS NMR measurements of the samples in fused glass ampoules were performed using an MSL 500 spectrometer with a MAS frequency of 10 kHz. Pulse lengths for the ^{1}H MAAS NMR Hahn echo experiments were $t_{\pi/2} = 4.5$ µs und $t_\pi = 9$ µs with a 1-ms delay between the two pulses. Dephasing of ^{27}Al (TRAPDOR) was performed by two 900-µs pulses with a mutation frequency of about 100 kHz. A 16-phase cycle was applied in the ^{1}H channel. The well-characterized dehydrated sample of H-ZSM-5 with a framework Si/Al ratio of 17 in a fused glass ampoule was used as a reference for the ^{1}H intensity measurements.

The one-dimensional ^{1}H MAS NMR exchange experiments were performed by the NOESY pulse sequence depending on the duration of the mixing period t_m. The frequency offset and the duration of the evolution period were adjusted to a maximum signal intensity of the bridging OH groups and to a minimum signal intensity of the benzene in the signal for $t_m = 4$ µs and were kept constant for all values of t_m. The exchange rates, $k = 1/\tau_{OH} + 1/\tau_{benzene}$, were obtained from the evaluation of the sum of relaxation matrixes and kinetic matrixes in a procedure described by Mildner and Freude [9]. The mean residence times of a hydrogen atom in a bridging hydroxyl group and a benzene molecule were denoted by τ_{OH} and $\tau_{benzene}$, respectively.

3. Results

3.1. ICP, BET, TPD, FTIR, and XRD characterization

Table 2 shows that, as expected, the bulk Si/Al ratio of 38 for product β was unchanged by the modification. BET surface and micropore volume increased significantly from procedure II to procedure III. The difference between step 3 and step 4 is not significant. NH_3-TPD measurements were used to calculate the total acidity (Brønsted and Lewis) by deconvolution of the NH_3-TPD spectra as described previously [20]. Comparing the FTIR signals at 1546 cm^{-1} (due to adsorption of pyridine at Brønsted acid sites) and 1444 cm^{-1} (due to adsorption of pyridine at Lewis acid sites) gives a relative measure of Brønsted and Lewis acidity in arbitrary units (see Table 2).

Table 2
Physico-chemical characterization. The chemical composition determined by ICP yields a sodium concentration less than 0.02 wt% for the products d and e and an iron concentration less than 0.01 wt% for all products. The surface area and the micropore volume were obtained by low temperature N_2 adsorption. The amount of acidity was determined by NH_3-TPD measurements. FTIR spectroscopy of pyridine loaded products gives a measure of Brønsted and Lewis acidity

Product	BET surface ($m^2\,g^{-1}$)	Micropore volume ($cm^3\,g^{-1}$)	Acidity 10^{-6} (mol g^{-1})	Brønsted acidity (a.u.)	Lewis acidity (a.u.)
βId	341	0.130	269	124	3
βIId	327	0.124	307	143	2
βIIId	379	0.148	212	82	3
βIe	355	0.129	107	42	13
βIIe	351	0.126	102	40	15
βIIIe	382	0.143	109	43	18

According to XRD analysis, all prepared products have a typical ZSM-5 diffraction pattern. Other crystalline phases were not found. As a relative measure of the crystallinity, we use the value Q_{Al} obtained from comparing XRD intensities of the MFI sample under study with those of the reference spectrum of aluminum oxide α-Al_2O_3 (corundum). The value Q_{Al} is defined as

$$Q_{Al} = \frac{2 \times I(\text{MFI}, 2\theta \approx 23.1^\circ)}{I(\text{corundum}, 2\theta = 35.2^\circ) + I(\text{corundum}, 2\theta = 43.1^\circ)},$$

where I denotes the intensity (height of the reflection peaks in counts/s) of the main X-ray reflections, MFI denotes the reflection of zeolite MFI under study, and corundum denotes the reflexes of the α-aluminum oxide reference sample, which has the same volume and is measured under the same conditions as the zeolite sample [21]. A Q_{Al} value around 1 corresponds to a fully crystalline product, whereas a value near 0 indicates an amorphous product. Fig. 1 shows the step-by-step crystallinity loss for the three modification procedures.

We note here that the chemical composition determined by ICP yields an iron concentration < 0.01 wt% for all products. The iron concentration $<$ of 100 ppm holds steady in all of the samples under study. Kubánek et al. [22] claimed that a dehydrated H-ZSM-5 zeolite with very low iron content (30 ppm Fe) exhibited almost no catalytic activity in benzene-to-phenol hydroxylation. Our study shows that significant variations in the catalytic activity occur for samples with different pretreatments but identical iron contents. Therefore, we discuss the influence of the iron content, which was clearly demonstrated by Kubánek et al. [22].

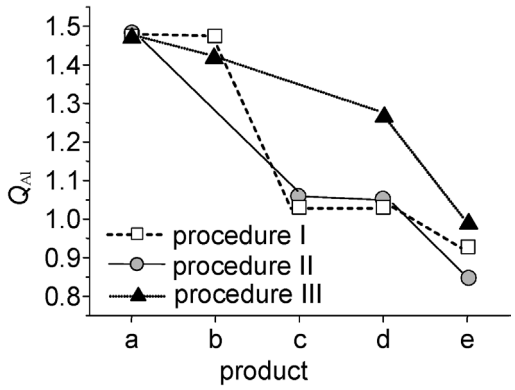

Fig. 1. Crystallinity of the zeolites after modification procedures for products β (high silicon-to-aluminum ratio).

Table 3
The N_2O conversion X_N, the benzene conversion X_B, the yield Y_P of phenol with respect to benzene, the selectivity $S_{P/B}$ of phenol with respect to benzene, and the selectivity $S_{P/N}$ of phenol with respect to N_2O. Values are given in mol%

Product	X_N (%)	Y_P (%)	$S_{P/B}$ (%)	X_B (%)	$S_{P/N}$ (%)
αId	12.7	6.7	52	12.9	53
αIId	8.3	5.1	62	8.2	61
αIIId	11.8	7.3	63	11.6	62
αIe	9.9	6.3	64	9.8	64
αIIe	12.3	9.9	81	12.2	80
αIIIe	12.2	9.2	90	10.2	75
βId	16.0	10.0	69	14.5	63
βIId	25.3	13.9	67	20.7	55
βIIId	11.5	7.0	75	9.3	61
βIe	30.1	18.1	80	22.6	60
βIIe	30.5	17.7	73	24.2	58
βIIIe	28.2	17.6	76	23.2	62

3.2. Catalytic tests

Direct benzene oxidation with N_2O was used as a catalytic test reaction. Table 3 presents the values of the N_2O conversion, X_N; the benzene conversion, X_B; the yield of phenol with respect to benzene, Y_P; the selectivity of phenol with respect to benzene, $S_{P/B}$; and the selectivity of phenol with respect to N_2O, $S_{P/N}$, for the three different treatment pathways (procedures I, II, and III).

Catalytic behavior cannot be explained by simple tendencies. Comparing two basic product types (zeolites with different Si/Al ratios) shows that in general, the performance values for the β products (higher Si/Al ratios) are higher than those for the α products (lower Si/Al ratios). In case of the α products (low Si/Al ratios), the activities (conversions) are nearly the same independent of calcination temperature; however, the selectivity ($S_{P/B}$) of d products (823 K) is higher for procedure III. The comparison of the calcination temperature shows higher values for the activities (X_N), yields (Y_P), and selectivites ($S_{P/B}$) at higher treatment temperatures. The values for products calcined at 1173 K (products e) do not depend significantly on the procedure.

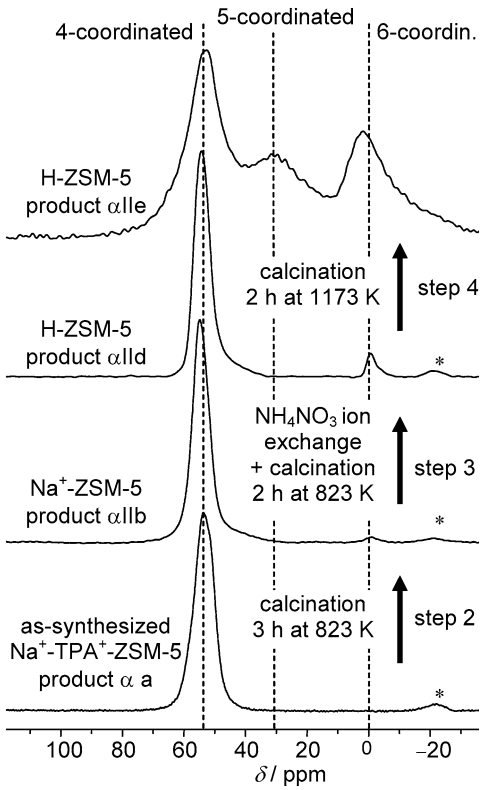

Fig. 2. ^{27}Al MAS NMR spectra of the products αII in dependence on the steps of modification. Asterisks denote spinning side bands. The resonance shifts correspond to the sum of isotropic chemical shift and isotropic quadrupole shift.

3.3. ^{27}Al and ^{29}Si NMR spectroscopy of the rehydrated samples

^{27}Al MAS NMR spectra of the rehydrated as-synthesized zeolites ZSM-5 and the reference product H-ZSM-5 consist of only one signal with an isotropic chemical shift ($\delta_{CS\ iso}$) of about 56 ppm. The thermal treatment gives rise to three additional signals: four-coordinated extra-framework aluminum atoms ($\delta_{CS\ iso} \approx 65$ ppm), fivefold-coordinated extra-framework aluminum atoms ($\delta_{CS\ iso} \approx 38$ ppm), and sixfold-coordinated extra-framework aluminum atoms ($\delta_{CS\ iso} \approx 10$ ppm); see Fig. 2. Fyfe et al. [23] found four additional signals in the spectra of hydrothermally treated zeolites Y (USY): fourfold-coordinated framework aluminum atoms ($\delta_{CS\ iso} = 60.7$ ppm, $C_{qcc} = 2.4$ MHz, $\eta = 0.53$), fourfold-coordinated extra-framework aluminum atoms ($\delta_{CS\ iso} = 60.4$ ppm, $C_{qcc} = 6.27$ MHz, $\eta = 0.1$), fivefold-coordinated extra-framework aluminum atoms ($\delta_{CS\ iso} = 32.2$ ppm, $C_{qcc} = 3.85$ MHz, $\eta = 0.1$), and sixfold-coordinated extra-framework aluminum atoms ($\delta_{CS\ iso} = 3.2$ ppm, $C_{qcc} = 3.28$ MHz, $\eta = 0.1$). Here C_{qcc} and η denote the quadrupole coupling constant and the asymmetry parameter, respectively.

The products pretreated at 1173 K contain the same concentrations of aluminum as the as-synthesized products (4.9 aluminum atoms per unit cell for product α a), but the aluminum concentration is distributed in 13 and 17% fourfold-coordinated framework aluminum, 28 and 30% fourfold-coordinated extra-framework aluminum, 28 and 33% fivefold-coordinated extra-

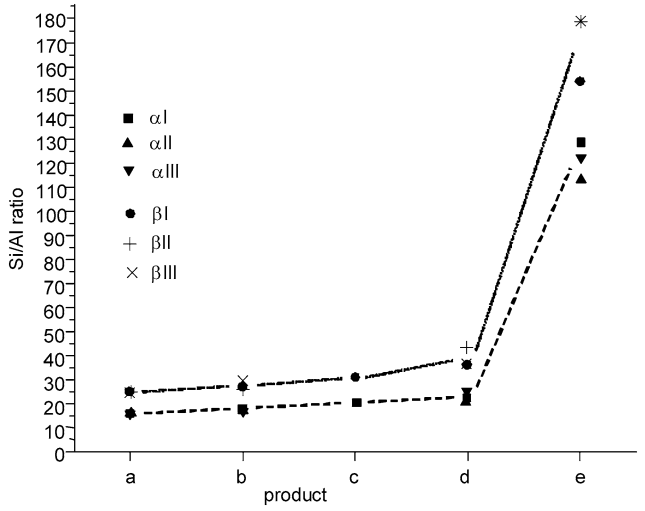

Fig. 3. The silicon-to-aluminum ratio obtained from the fit of the signal of the framework aluminum in the ^{27}Al MAS NMR spectra of the rehydrated samples under study in comparison to a test sample. The experimental error is ±10%.

framework aluminum, and 31 and 20% sixfold-coordinated extra-framework aluminum for products αIe and βIe, respectively; see Table 5. Fivefold-coordinated extra-framework aluminum species can be observed only in those rehydrated products calcined at 1173 K. The concentrations of fivefold-coordinated species per unit cell of the rehydrated zeolite are 1.6 for product αIe, 1.1 for product αIIe, 0.9 for product αIIIe, 1.2 for product βIe, 0.4 for product βIie, and 0.4 for product βIIIe.

Framework Si/Al ratios were obtained from the fit of the signal of the framework aluminum in the ^{27}Al MAS NMR spectra of the rehydrated samples under study in comparison with a well-characterized test sample with a Si/Al ratio of 17. Results are presented in Fig. 3. The as-synthesized sample α has a ratio of 16, which increases to 128 for step 4 and procedure I. The as-synthesized sample β has a ratio of 25, which increases to 179 for step 4 and procedure III. A significant difference due to the treatment procedures I, II, and III cannot be observed, because the experimental error is ±10%.

Fitting the experimentally obtained spectra using the dmfit program [19] requires two types of signals for sixfold-coordinated extra-framework aluminum species, with $\delta_{\mathrm{CS\ iso}} = 7$ ppm and $\delta_{\mathrm{CS\ iso}} = 13$ ppm instead of one signal at $\delta_{\mathrm{CS\ iso}} \approx 10$ ppm. The set of NMR data presented in Table 4 gives mean values of the NMR parameters obtained from the fit of all ^{27}Al MAS NMR spectra measured in the field of 11.74 T ($\nu_{\mathrm{L}} = 130$ MHz).

The simulation software dmfit [19] includes a Gaussian broadening of the signals. This fits well with a Gaussian distribution of the isotropic chemical shift and less exactly with a distribution of quadrupole parameters. The broadening parameter applied to the spectra obtained at $\nu_{\mathrm{L}} = 130$ MHz corresponds to a Gaussian distribution of isotropic chemical shifts with a full width at half maximum (fwhm) $\Delta\delta_{\mathrm{CS\ iso}}$ in the interval of 8–30 ppm; see Table 4. The ratio of chemical shift broadening to second-order quadrupole broadening increases with increasing square of the external magnetic field. But the

Table 4
The parameters $\delta_{\mathrm{CS\ iso}}$, C_{qcc} und η of the ^{27}Al MAS NMR spectra

Aluminum species	$\delta_{\mathrm{CS\ iso}}$ (ppm)	$\Delta\delta_{\mathrm{CS\ iso}}$ (ppm)	C_{qcc} (MHz)	η
Fourfold-coordinated extra-framework	65 ± 2	8 ± 1	6.6 ± 0.2	0.20 ± 0.1
Fourfold-coordinated framework	56 ± 2	20 ± 2	3.4 ± 0.2	0.6 ± 0.1
Fivefold-coordinated extra-framework	38 ± 2	30 ± 4	4.8 ± 0.2	0.5 ± 0.1
Sixfold-coordinated extra-framework	13 ± 2	8 ± 1	6.8 ± 0.2	0.2 ± 0.1
Sixfold-coordinated extra-framework	7 ± 2	15 ± 2	4.0 ± 0.2	0.6 ± 0.1

Table 5
Relative concentrations of aluminum species for the hydrated products calcined before at 1173 K

Species	αIe	βIe
Fourfold-coordinated framework aluminum $\delta_{\mathrm{CS\ iso}} \approx 56$ ppm	13%	17%
Fourfold-coordinated extra-framework aluminum $\delta_{\mathrm{CS\ iso}} \approx 65$ ppm	28%	30%
Fivefold-coordinated extra-framework aluminum $\delta_{\mathrm{CS\ iso}} \approx 38$ ppm	28%	33%
Sixfold-coordinated extra-framework aluminum $\delta_{\mathrm{CS\ iso}} \approx 10$ ppm	31%	20%

quadrupole parameters, C_{qcc} and η, and the chemical shift parameters, $\delta_{\mathrm{CS\ iso}}$ and $\Delta\delta_{\mathrm{CS\ iso}}$, do not depend on the external magnetic field. Fig. 4 shows the MAS NMR and 3QMAS NMR spectra of product αIIIe measured at $\nu_{\mathrm{L}} = 195$ MHz. Fitting the MAS spectrum by five signals also yields the parameters given in Table 4. This confirms the values presented in Table 4, which were based on the experiments with a Larmor frequency of $\nu_{\mathrm{L}} = 130$ MHz. Particularly, the signal in the middle of the ^{27}Al MAS NMR spectra of the rehydrated products treated at 1173 K has an isotropic chemical shift of 38 ppm and should be assigned to fivefold-coordinated aluminum species.

^{29}Si MAS NMR spectra of the samples under study (not shown here) exhibit no broadening (but even a narrowing by 15%, due to framework dealumination) of the signals on thermal treatment up to 1173 K. This proves that the thermal treatment does not destroy the near-range order of the zeolite. The ^{29}Si MAS NMR line shape analysis gives Si/Al ratios of 16 and 25 for the as-synthesized ZSM-5 products α and β, respectively.

3.4. *^{1}H MAS NMR spectra of the dehydrated products without and with ^{27}Al dephasing*

Fig. 5A shows the usual ^{1}H MAS NMR spectra. The spectra in the middle [Fig. 5B] were measured with ^{27}Al irradiation (TRAPDOR) [6]. Signals of hydrogen nuclei that are dipolar coupled to aluminum nuclei are quenched in the spectra in Fig. 5B, whereas the difference spectra in Fig. 5C consists only of those signals. Thus the usual spectra A are divided into two parts: B, giving the signals of hydroxyl groups that are far from aluminum nuclei, and C, showing the signals of hydroxyl

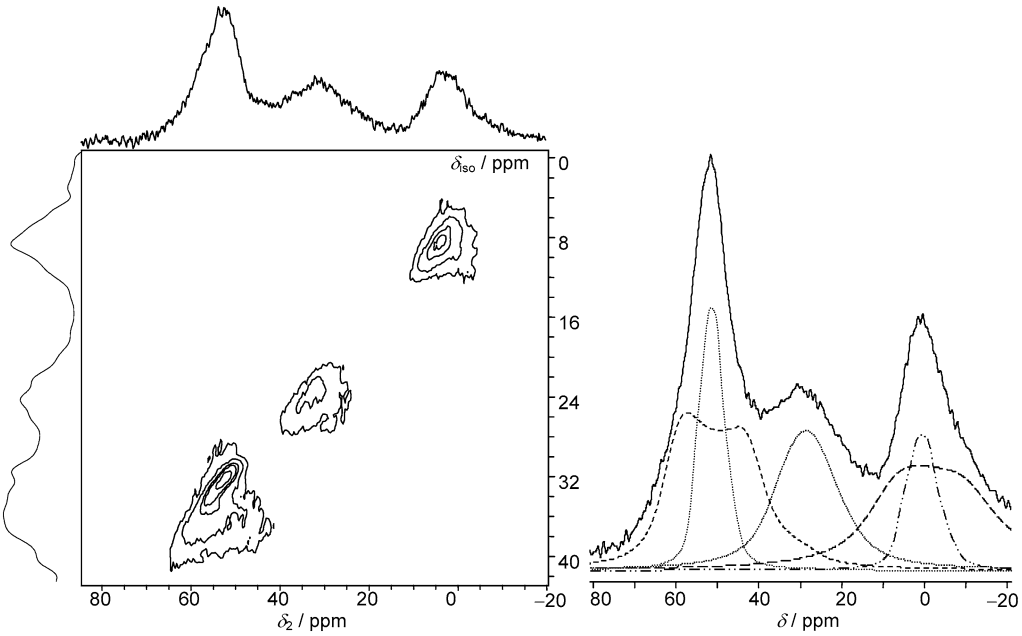

Fig. 4. ^{27}Al MAS NMR and ^{27}Al 3QMAS NMR spectra of product αIIIe measured at $\nu_L = 195$ MHz and $\nu_{rot} = 30$ kHz. The four dashed lines in the MAS fit correspond to the species listed in Table 4.

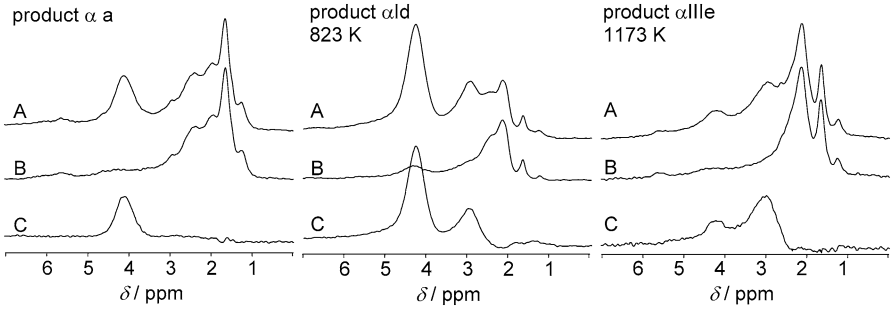

Fig. 5. ^{1}H MAS spectra of dehydrated products α as-synthesized, αId and αIIIe showing the influence of the thermal treatment. The spectra on the top (A) show the usual ^{1}H MAS NMR spectra, the spectra in the middle (B) are measured with ^{27}Al irradiation (TRAPDOR) and the spectra on the bottom (C) are difference spectra (A) − (B). The intensities of the spectra of product αId had to be increased by factor 2, in order to make their intensities comparable to those of the other spectra.

groups in the neighborhood of aluminum nuclei (≡SiOHAl≡ and =AlOH species).

The spectra depicted in Fig. 5 show signals at 4.2–4.4 ppm due to bridging hydroxyl groups (≡SiO^{H}Al≡); signals at 2.9 ppm due to extra-framework AlOH groups, which have a weak hydrogen bond to framework oxygen atoms; and several signals in the region of 1.5–2.2 ppm due to SiOH groups on framework defects [3,4]. Concentrations of species per unit cell are 1.1 ± 0.2, 0.0, and 1.2 ± 0.2 for the species SiO^{H}Al, AlOH and SiOH, respectively in product α a (as-synthesized product); 3.3 ± 0.6, 1.0 ± 0.2, and 0.7 ± 0.2, respectively, in product αId; and 0.7 ± 0.2, 0.8 ± 0.2, and 1.0 ± 0.2, respectively, in product αIIIe. The dehydration procedure (Section 2.3) can be considered mild calcination. Therefore, it is not surprising that a low concentration (1.1 species per unit cell) of bridging hydroxyl groups is found in product αa. This concentration increases after the usual calcination and ammonium exchange and repeated calcination at 823 K (product αId) up to 3.3 species per unit cell. The spectrum of this product shows also a signal of AlOH groups for which the concentration is 1.0 species per unit cell. For the product calcined at 1173 K (product αIIIe), the concentration of the AlOH is reduced to 0.8 species per unit cell, whereas the concentration of bridging hydroxyl groups decreases more significantly, to 0.7 species per unit cell, and the concentration of defect silanol groups increases to 1.0 per unit cell.

3.5. ^{1}H MAS NMR exchange spectroscopy

The ^{1}H MAS chemical shift of bridging hydroxyl groups can be considered a measure of acid strength [3], but the small shift range from 4.2 ± 0.1 ppm to 4.4 ± 0.1 ppm on framework dealumination (see Fig. 5) does not provide significant evidence of enhanced acid strength. Therefore, we use the temperature-dependent proton exchange rate between bridging hydroxyl groups and adsorbed molecules of benzene as a dynamic measure of Brønsted acidity [9]. Dehydrated samples were loaded with 1.3 benzene molecules per unit cell and investigated by ^{1}H MAS NMR with a NOESY (nuclear Overhauser effect spectroscopy) pulse sequence. The strong temperature dependence

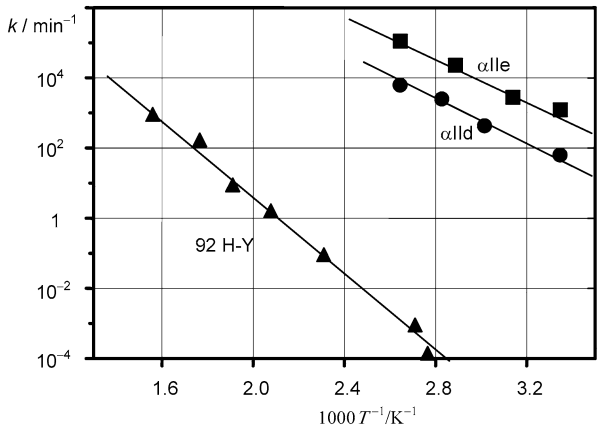

Fig. 6. Arrhenius plot $k = k_0 \exp(-E_A/RT)$ of the hydrogen exchange rates in the benzene loaded hydrogen forms of zeolites. Zeolites αIId and αIIe were treated at 823 and 1173 K, respectively. The values for the zeolite 92 H-Y, which was calcined under mild conditions below 723 K, were taken from Ref. [9].

(see Fig. 6) shows that the magnetization transfer between hydrogen nuclei was caused by chemical exchange and not by spin–spin coupling.

Fig. 6 shows that the rates of the proton transfer between bridging hydroxyl groups and benzene molecules in the temperature region 300–380 K (temperature of the NMR experiment) increase by a factor of ca. 7 after increasing the treatment temperature from 823 to 1173 K. It was not possible to measure exchange rates for a template-free synthesized and HCl acid-treated (but noncalcined) zeolite H-ZSM-5, because the H/D exchange was too fast (even at room temperature) to allow the observation of the time-dependent H/D exchange. Moreover, the exchange rates by chemical exchange were smaller than those by spin diffusion at higher temperatures. Therefore, we present data obtained for a zeolite H-Y [9] for comparison.

4. Discussion

4.1. Synthesis and modification

Fig. 1 shows that the acidic treatment (treatment steps 1) in procedures I and III that was been added to the standard procedure (II) does not influence the crystallinity of the products, indicating that the structure remains intact after this treatment step. However, a drastically decreased crystallinity is observed after calcination at 823 K (step 2) for the products c of procedures I and II. This is due to the removal of the template from the pore system of the products. Interestingly, these values are similar to values that we obtained for products synthesized in template-free crystallizations in an earlier study [11]. Pathways I and II yield products d as catalytically active H forms (after template removal and the ion exchange), for which no significant further decrease of the crystallinity value is observed in step 4. But pathway III yields the product d (after a combined ion-exchange and calcination procedure) with a relatively high crystallinity (Q_{Al} value of ca. 1.3) for a template-free H form of an MFI zeolite. This might be due to the lowered alkalinity of the product during the first calcination step. Calcination at a higher temperature of 1173 K (step 4) leads to a first destruction of the long-range order with the best result for procedure III ($Q_{Al} = 0.99$). Procedure II (the product after the standard recipe without an acidic pretreatment) leads to products with the lowest crystallinity ($Q_{Al} = 0.85$). However, it should be emphasized that even the value $Q_{Al} = 0.85$ represents good crystallinity. The values of the BET surface areas and micropore volumes confirm both good crystallinity for all products and a slight decrease after modification; see Table 2.

The ^{27}Al MAS NMR intensity measurements give Si/Al ratios of 16 and 25 for the as-synthesized ZSM-5 products α and β, respectively, in agreement with the ^{29}Si MAS NMR line shape analysis. The increase in the framework Si/Al ratio is presented in Fig. 3. Calcination at 823 K causes an approximate 50% increase in the Si/Al ratio. A strong framework dealumination and increase of the Si/Al ratio by a factor of about 7 with respect to the as-synthesized material occurs during calcination at 1173 K. Sodium ions, which are more thermally stable than ammonium ions, are removed before step 4, allowing the strong dealumination during step 4.

We have proven that the total amount of aluminum in the products remains constant within the ±10% limit of experimental accuracy. This means that the products pretreated at 1173 K contain the same concentrations of aluminum as the as-synthesized products (5.65 and 3.69 aluminum atoms per unit cell for products α and β, respectively), but the aluminum concentration is distributed in 13 and 17% fourfold-coordinated framework aluminum, 28 and 30% fourfold-coordinated extra-framework aluminum, 28 and 33% fivefold-coordinated extra-framework aluminum, and 31 and 20% sixfold-coordinated extra-framework aluminum for products αIe and βIe, respectively. We again mention that this quantitative characterization concerns the hydrate zeolites, whereas dehydrated (activated) zeolites are used for catalysis. A remarkable number of Lewis acid sites can be observed after calcination at 1173 K, whereas the concentration of Brønsted acid sites decreases significantly during step 4; see Table 2.

4.2. Catalysis

Treatment procedures I and III involve acidic leaching before the samples are stressed by thermal treatment. A partial reduction in sodium content could have taken place before template removal. This can be the reason for the higher thermal stability, which can be concluded from the higher crystallinity (Q_{Al} values) of samples d and e after the thermal treatment; see Fig. 1. With decreasing alkaline excess in the procedure I and III, we found a decreasing N_2O conversion from X_N (25.3 (II) to 16.0 (I) and 11.5 (III)) and benzene conversion from X_B (20.7 (II) to 14.5 (I) and 9.3 (III)) for the β products after treatment step d. For the β products, after treatment at 1173 K, this difference is very small (e.g., 30.5 (II), 30.1 (I), and 28.2 (III) for X_N). Similar changes in the phenol yields can be observed for the treatment at 873 K (13.9 (II), 10.0 (I), and 7.0 (III)) and for the treatment at 1173 K (17.7 (II), 18.1 (I), and 17.6 (III)); see Table 3. Due to decreasing catalytic activity for the β products at 873 K, the selectivities $S_{P/B}$ are improved, from 67 (II) to 69 (I) and 75 (III). This behavior of

the β products treated at 873 K correlates with the changes in Brønsted acidity; increasing acidity results in an increased conversion. After calcination at 1173 K, all products have higher but similar catalytic activities due to the same level of Brønsted acidity; see Table 2. This means that on the one hand, different treatment procedures give similar results, because structural differences that might be implemented by the different procedures are equalized in respect to their catalytic functions by the thermal treatment at 1173 K, but on the other hand, despite the drastically reduced Brønsted acidity, the conversions (X_N and X_B) and yields (Y_P) are significantly increased compared with the products treated at lower temperatures. This might indicate that the number of active sites is not the most important factor in the performance of benzene hydroxylation. The small increase in Lewis acidity with increasing temperature of treatment cannot completely explain this increase in catalytic values. A possible combination of Lewis and Brønsted sites after treatment may be the source of the improved performance.

Unfortunately, we cannot yet explain the exceptionally high selectivity values ($S_{P/B}$) of about 80 for product αIIe and 90 for product αIIIe. We can, however, note that the concentrations for the fivefold-coordinated species with 1.1 and 0.9 species per unit cell are nearly at the same level (see Section 4.3).

Based on the foregoing findings, some general trends can be derived:

1. The highest values of the characteristic catalytic key data (X, Y) are obtained for the products treated at 1173 K, independent of the treatment stage (product d or e) and the α or β product (procedure I, II, or III).
2. Comparing products with the different Si/Al ratios: the products with the lower Al content are more active (i.e., higher conversions and yields) for benzene hydroxylation to phenol.

Interestingly, in the preparation of an effective catalyst for the described test reaction, for the products with lower Si/Al ratios, procedure III is more effective, whereas for the products with higher Si/Al ratios, procedure I seems preferable. Note that selectivities ($S_{P/B}$) equal or higher than 80% are associated with a concentration of about one fivefold-coordinated aluminum atom per unit cell (see Section 4.3).

From the foregoing observations, we must conclude that describing the catalyst preparation procedure in a precise manner is very important. On the other hand, choosing a special treatment procedure allows for the adjustment and design of special catalyst properties even when a single-parent zeolite is used. Furthermore, starting with different zeolites, the same procedure leads to products with different catalytic properties. Finally, one must assume that the catalytically active centers on or in the zeolite are complex arrangements involving differently structured species.

4.3. Nature of active sites

The ^{27}Al MAS NMR intensity measurements of the samples under study gave two remarkable results. The first result is that, as expected, the framework Si/Al ratio strongly increased on thermal treatment (see Figs. 4 and 5), whereas sixfold- and fourfold-coordinated extra-framework aluminum species are created. The second result is that fivefold-coordinated extra-framework aluminum species can be found in the rehydrated samples of product e (calcined at 1173 K). The concentrations of fivefold-coordinated species per unit cell were 1.6 for product αIe, 1.1 for product αIIe, 0.9 for product αIIIe, 1.2 for product βIe, 0.4 for product βIIe, and 0.4 for product βIIIe.

Deng et al. [24] could not find fivefold-coordinated aluminum species in rehydrated zeolites at treatment temperatures up to 973 K. In the ^{27}Al MAS NMR spectra of our products, which were treated at 823 K, the signal of fivefold-coordinated species is missing as well. The increased yield, Y, and selectivity, S, of phenol with respect to benzene after sample treatment at 1173 K (see Table 3) focuses our attention on the fivefold-coordinated aluminum species. Note that the ^{27}Al NMR spectrum of a *dehydrated* zeolite H-ZSM-5 is very broad, with a spectrum width of about 800 ppm at $\nu_L = 130$ MHz [25] as opposed to a spectrum width of about 80 ppm for hydrated samples. Therefore, signals with different chemical shifts cannot be resolved in the spectra of dehydrated zeolites. But all catalysts are dehydrated after the activation procedure in a catalytic process. The crucial point of the present discussion is that the very symmetrical extra-framework species (which give rise to the resolved signals in the NMR spectra) exist only in the *hydrated* zeolite, probably in water coordination. But their nature can be changed or their symmetry disturbed in the *dehydrated* form of the zeolite.

The nature of extra-framework aluminum species remains speculative and controversial. Threefold-coordinated aluminum atoms (Lewis sites) in the zeolitic framework have been discussed in many publications since the corresponding proposal of Uytterhoeven et al. [26], but they can hardly build a highly symmetric fivefold-coordinated complex with water molecules. Therefore, it seems certain that this complex is an extra-framework compound or is connected to a defect of the framework.

Consider three of the proposed species. The arrangement ≡SiOAlOH represents a hydroxyl group on a framework defect in the dehydrated zeolite. This non-framework site is still connected to the framework via the SiOAl bridge. On hydration, the attachment of three water oxygen atoms to the aluminum atom creates a fivefold-coordinated aluminum species. Another example is an Al_2O_3 compound in the calcined and dehydrated zeolite that has no connection to the framework. On rehydration, it can be transformed to $Al(OH)_3$ molecules, and the further attachment of two water molecules gives a fivefold-coordinated extra-framework aluminum species. A charged species is the cation $Al(OH)_2^+$ in the dehydrated zeolite, which can be transformed into a fivefold-coordinated cation by the attachment of three water molecules on hydration. The latter requires a charge compensation by framework aluminum atoms that are not part of a Brønsted site ≡SiO^{H}Al≡. But fewer than one framework aluminum atom exists in the unit cell of the ZSM-5 zeolite for Si/Al > 95. The concentration of framework aluminum atoms can be calculated from the Si/Al ratios given in Fig. 3; for

example, 0.82 ± 0.1 aluminum atoms per unit cell exist at a Si/Al ratio of 114 in product αIIIe. The values obtained thusly are comparable with the concentrations of Brønsted sites determined by ^{1}H MAS NMR, for eample, 0.7 ± 0.2 per unit cell in product αIIIe. Therefore, charged extra-framework aluminum species can be excluded as a source of the fivefold-coordinated species, which have a concentration of 0.9 per unit cell for product αIIIe. Small Al_2O_3 compounds cannot be excluded as the source of fivefold-coordinated species on rehydration, but with our numbers it seems more likely that ≡SiOAlOH species play this role, because the concentration of 0.8 ± 0.2 AlOH groups for the dehydrated product αIIIe agrees well with the concentration of 0.9 fivefold-coordinated species of the hydrated sample.

Such an explanation implies a different nature of AlOH groups in products d and e, however. Only the latter create fivefold-coordinated species on rehydration. The concentration of AlOH groups found in the ^{1}H MAS NMR spectra is only slightly higher at a treatment temperature of 823 K than at 1173 K. But if we consider the AlOH species in products d (1.0 ± 0.2 in product αId) as charged cations, $AlOH^{2+}$, then the concentration of framework aluminum atoms (4.8 ± 0.4 per unit cell in product αId) minus the concentration of Brønsted sites (3.3 ± 0.6 in product αId) is not far from twice the concentration of $AlOH^{2+}$ cations. A possible explanation for this finding is that step 3 results in AlOH groups as $AlOH^{2+}$ cations with hydrogen atoms pointing to framework oxygen atoms, whereas step 4 creates hydroxyl groups in the form of ≡SiOAlOH that create fivefold-coordinated aluminum species on rehydration.

The concept of dissociated aluminum sites in the ZSM-5 framework was introduced by Haag et al. [27]. They proposed that one member of a paired Al region is modified during steaming, possibly partially hydrolyzed, and acts as a strong electron-withdrawing center for the remaining tetrahedral Al, thus creating a stronger Brønsted site [27]. This was discussed in the context of enhanced catalytic activity after mild steaming, but fivefold-coordinated aluminum species cannot found after mild steaming, performed at about 800 K and under weak additional water pressure [27]. At 1173 K, the self-steaming water pressure is very low, defects in the framework cannot heal, and extra-framework aluminum species hardly condense. Therefore, we should not exclude the discussion of hydrated fivefold-coordinated aluminum species arising from small Al_2O_3 species in the dehydrated zeolite. The smallest Al_2O_3 compound is an Al_2O_3 molecule, which under rehydration gives two $Al(OH)_3$ species with two attached water molecules for each. The Al_2O_3 molecules exist in the dehydrated sample of two threefold-coordinated aluminum atoms with Lewis acid properties. They could also be considered a source of a special catalyst property.

The cooperative effect of all of these different species for catalysis is very complex and not yet clear. The contributions of other species not mentioned above cannot be excluded.

The framework dealumination causes only a small change of the chemical shift of the bridging hydroxyl groups of <0.2 ppm, but it has a strong influence on the proton transfer, which can be considered a dynamic measure of Brønsted acidity [28]. Apparent activation energies were obtained from a linear fit of the Arrhenius plot of the temperature-dependent hydrogen exchange rates between bridging hydroxyl groups and adsorbed benzene molecules (1.3 benzene molecules per unit cell), which are ca. 55 and 50 kJ mol^{-1} for products α1d and α1e, respectively, significantly less than the apparent activation energy of 93 kJ mol^{-1} for slightly dealuminated zeolite H-Y [9]. It is remarkable that the Arrhenius plot of the samples in this study and the samples studied in earlier work [9] yield a pre-exponential factor of 3×10^9 s^{-1}, nearly equal to the rotational constant of 2.8×10^9 s^{-1} for the benzene rotation (about the C_6 axis) [29], whereas the stretching vibration of the bridging hydroxyl groups is about 10^{14} Hz. This provides a clue that the rotation of the molecule may play a role in proton transfer. But the main messages from Fig. 6 are that at about 380 K, the hydrogen exchange rate of our products d end e is more than six orders of magnitude higher than those obtained for a slightly dealuminated zeolite H-Y and, comparing products αIId and αIIe, step 4 increases the hydrogen exchange rate by more than one order of magnitude. The latter fact seems to be temperature-independent in the observed range 300–380 K. The decreased activation temperature and increased hydrogen exchange rate by step 4 of the catalyst treatment procedure is remarkable. Hydrogen exchange needs Brønsted sites. The main spectroscopic result of this study is the demonstrated change in the aluminum sites after strong calcination. Therefore, an explanation by combined actions of Brønsted and Lewis sites for the catalytic reaction seems plausible, but is not yet supported by an exact model of the nature of such sites.

5. Conclusion

^{29}Si MAS NMR spectra of the samples under study show no broadening (with even a 15% narrowing due to framework dealumination) of the signals on thermal treatment up to 1173 K. This proves that the thermal treatment does not destroy the near-range order of the zeolite.

^{27}Al MAS NMR and ^{27}Al 3QMAS NMR studies of the samples give evidence that fivefold-coordinated aluminum species exist if the product is treated at 1173 K and then rehydrated. The nature of this species is not yet clear. Two models are in agreement with our experimental findings. The arrangement ≡SiOAlOH represents a hydroxyl group on a framework defect in the dehydrated zeolite. This nonframework site is still connected to the framework via the SiOAl bridge. On hydration, the attachment of three water oxygen atoms to the aluminum atom creates a fivefold-coordinated aluminum species. Another model is an Al_2O_3 molecule in the calcined and dehydrated zeolite, which has no connection to the framework. On rehydration, it can be transformed to $Al(OH)_3$ molecules, and the further attachment of two water molecules gives a fivefold-coordinated extra-framework aluminum species.

Apparent activation energies of the hydrogen-exchange rate in benzene-loaded samples are ca. 55 and 50 kJ mol^{-1} for products pretreated at 823 K and 1173, respectively. Step 4 increases the hydrogen exchange rate by more than one order of magnitude. The main spectroscopic finding in this study is the change of the aluminum sites after strong calcination. An explanation

for the catalytic reaction involving combined actions of Brønsted and Lewis sites seems plausible, but is not yet supported by an exact model of the nature of such sites.

Interestingly, the differences with respect to the treatment procedures are more obvious at a calcination temperature of 873 K. For the N_2O conversions (X_N) and yields (Y_P), this effect can be correlated with differences in Brønsted acidity. After calcination at 1173 K, all products have nearly the same catalytic activity (conversion and yield), which correlates with the same level of Brønsted acidity after treatment. However, the values of all characteristic catalytic key data (X_N and Y_P) are highest when the catalysts are precalcined at 1173 K, independently from procedure I, II, or III.

In the catalytic reaction, the products prepared according to procedure III have the highest selectivities of phenol with respect to benzene: 63–52% and 62% for product αXd, 90–64% and 81% for product αXe, and 75–69% and 67% for product βXd.

Acknowledgments

We thank Dr. Jörg Kärger and Godwin T.P. Mabande for their helpful advice. This work was supported by the Deutsche Forschungsgemeinschaft (project Fr 902/12-1), the Max-Buchner-Stiftung, and the Fond der Chemischen Industrie.

References

[1] J. Weitkamp, L. Puppe, Catalysis and Zeolites, Springer, Berlin Heidelberg, 1999.
[2] G. Ertl, H. Knötzinger, J. Weitkamp, Handbook of Heterogeneous Catalysis, Wiley–VCH, Chichester, 1997.
[3] M. Hunger, Catal. Rev.-Sci. Eng. 39 (1997) 345.
[4] D. Freude, J. Kärger, in: F. Schüth, K. Sing, J. Weitkamp (Eds.), Handbook of Porous Materials, vol. 1, Wiley–VCH, Chichester, 2002, p. 465.
[5] C.A. Fyfe, J.L. Bretherton, L.Y. Lam, J. Am. Chem. Soc. 123 (2001) 5285.
[6] C.P. Grey, A.J. Vega, J. Am. Chem. Soc. 117 (1995) 8232.
[7] D. Freude, Chem. Phys. Lett. 235 (1995) 69.
[8] J. Kanellopoulos, Diploma thesis, Universität Leipzig, Leipzig, 2001.
[9] T. Mildner, D. Freude, J. Catal. 178 (1998) 309.
[10] A. Reitzmann, Ph.D. thesis, Universität Erlangen-Nürnberg, Erlangen, 2001.
[11] W. Schwieger, Habilitation thesis, Martin-Luther-Universität Halle-Wittemberg, Halle, 1994.
[12] W. Schwieger, K.H. Bergk, E. Alsdorf, H. Fichtnerschmittler, E. Loffler, U. Lohse, B. Parlitz, Z. Phys. Chemie (Leipzig) 271 (1990) 243.
[13] M. Soulard, S. Bilger, H. Kessler, J.L. Guth, Zeolites 7 (1987) 463.
[14] P.A. Jacobs, B.J. Uytterhoeven, J. Catal. 26 (1972) 175.
[15] V.R. Choudhary, S.G. Pataskar, Thermochim. Acta 97 (1986) 1.
[16] E. Alsdorf, M. Feist, T. Gross, H.J. Jerschkewitz, U. Lohse, M. Schwieger, Z. Phys. Chemie (Leipzig) 271 (1990) 267.
[17] J.L. Motz, H. Heinichen, W.F. Hölderich, J. Mol. Catal. A: Chem. 136 (1998) 175.
[18] L.M. Kustov, A.L. Tarasov, V.I. Bogdan, A.A. Tyrlov, J.W. Fulmer, Catal. Today 61 (2000) 123.
[19] D. Massiot, F. Fayon, M. Capron, I. King, S. Le Calve, B. Alonso, J.O. Durand, B. Bujoli, Z.H. Gan, G. Hoatson, Magn. Reson. Chem. 40 (2002) 70.
[20] F. Arena, R. Dario, A. Parmaliana, Appl. Catal. A: Gen. 170 (1998) 127.
[21] F. Scheffler, W. Schwieger, D. Freude, H. Liu, W. Heyer, F. Janowski, Microporous Mesoporous Mater. 55 (2002) 181.
[22] P. Kubanek, B. Wichterlova, Z. Sobalik, J. Catal. 211 (2002) 109.
[23] C.A. Fyfe, J.L. Bretherton, L.Y. Lam, Chem. Commun. (2000) 1575.
[24] F. Deng, Y.R. Du, C.H. Ye, J.Z. Wang, T.T. Ding, H.X. Li, J. Phys. Chem. 99 (1995) 15208.
[25] D. Freude, H. Ernst, I. Wolf, Solid State NMR 3 (1994) 271.
[26] J.B. Uytterhoeven, L.G. Christner, W.H. Hall, J. Phys. Chem. 69 (1965) 2117.
[27] R.M. Lago, W.O. Haag, R.J. Mikovsky, D.H. Olson, S.H. Hellring, K.D. Schmitt, G.T. Kerr, Stud. Surf. Sci. Catal. 28 (1986) 677.
[28] D. Freude, W. Oehme, H. Schmiedel, B. Staudte, J. Catal. 32 (1974) 137.
[29] Landolt-Börnstein, New Series II, vol. 19a, Springer, Berlin, 1992, p. 121.